A DFT Study of the Al_2O_3 Atomic Layer Deposition on SAMs: Effect of SAM Termination

Ye Xu[†] and Charles B. Musgrave*[,†,‡]

Departments of Materials Science and Engineering and Chemical Engineering, Stanford University, Stanford, California 94305-5025

Received October 14, 2003. Revised Manuscript Received December 1, 2003

The atomistic mechanism of the initial atomic layer deposition (ALD) reaction of trimethylaluminum [$Al(CH_3)_3$, TMA] on octadecyltrichlorosilane (OTS)-based self-assembled monolayers (SAMs) with different functional termination groups was investigated using density functional theory (DFT). The adsorption of TMA on $-NH_2$-terminated OTS involves formation of a dative bond between the amine lone pair and the Al atom of TMA and is exothermic by 0.86 eV. Conversion of the dative bond to a covalent bond through a four-centered H transfer from the NH_2 to the methyl group of TMA to form methane involves a barrier that is 1.22 eV above the adsorbed complex and is exothermic by 0.94 eV. Reaction between TMA and the −OH-terminated SAM results in an adsorption energy of 0.60 eV. Although the dative bond is weaker, the barrier to converting the dative bond to a covalent bond to form methane is only 0.65 eV relative to the complex structure and the overall reaction is exothermic by 1.44 eV. The reaction of TMA with the methyl-terminated SAM forms no adsorbed complex and the ligand exchange reaction to form methane requires a barrier of 1.82 eV and is endothermic by 0.09 eV. These results indicate that the end group of the SAM significantly affects the selectivity toward TMA adsorption and subsequent ALD of Al_2O_3. Although initiation of ALD reactions involving TMA appears to require lone pairs, even strong dative bonds, such as those between amine groups and TMA, lead to ligand exchange reactions that are not kinetically favorable.

Introduction

ALD was pioneered over 30 years ago by Suntola and co-workers and has since been investigated as a method for depositing thin films of a large number of different materials.[1] The ALD process involves the alternate exposure of a surface to gas-phase reactants that react to deposit at most a single monolayer of material on the surface for each exposure. The monolayer-by-monolayer nature of the deposition depends on the adsorption process reaching saturation at a single layer of precursor. Additional layers are deposited with subsequent pulses. To achieve self-limited growth, the precursor and surface functionalization must be chosen so that the precursor reacts only with the surface termination but not itself. ALD of various metal oxides has been studied because of their potential uses as dielectric materials and catalysts. In the case of metal oxides, two precursors are generally used, one acting as the metal source and the other as the oxygen source.[2] It is generally thought that surfaces must be terminated with hydroxyl groups to initiate the ALD of metal oxides upon exposure of the metal source.[3,4]

Another potential application of ALD is to deposit thin films onto various materials to control their surface properties. Self-assembled monolayers (SAMs) are interesting from this point of view for several reasons. For example, the ordered structure of the monolayer may act as a template for the growth of ordered films. Furthermore, the SAM may be used to control the properties of the interface to the underlying substrate, while the ALD coating could be used to protect the SAM. SAMs have also been investigated as potential ALD masks, although in this application the ALD reactions on the SAM are not desirable.[5,6] Similarly, ALD of films on polymers is of general interest because it enables the potential for applying extremely thin films on the polymer which might act as protecting layers or optical coatings or possibly control the surface functionality to bestow specific properties to the polymer surface. For example, ALD of a thin metal or metal oxide film on a SAM or organic film might enable control of the interface properties when forming metal contacts to an organic electronic device, such as field-effect transistors,[7] organic light-emitting diodes,[8] and photovoltaics.[9]

* To whom correspondence should be addressed. E-mail: charles@chemeng.stanford.edu.
[†] Department of Materials Science and Engineering.
[‡] Department of Chemical Engineering.

(1) Suntola, T.; Hyvarinen, J. *Annu. Rev. Mater. Sci.* **1985**, *15*, 177.
(2) Leskela, M.; Ritala, M. *Thin Solid Films* **2002**, *409*, 138.
(3) Haukka, S.; Lakomaa, E.; Root, A. *J. Phys. Chem.* **1993**, *97*, 5085.
(4) Matero, R.; Rahtu, A.; Ritala, M.; Leskela, M.; Sajavaara, T. *Thin Solid Films* **2000**, *368*, 1.
(5) Yan, M.; Koide, Y.; Babcock, J.; Markworth, P.; Belot, J.; Marks, T.; Chang, R. *Appl. Phys. Lett.* **2001**, *79*, 1709.
(6) Chen, R.; Kim, H.; Mcintyre, P. C.; Bent, S. F. To be submitted.
(7) Hwang, S.; Yu, Y.; Ha, W.; Kim, T.; Han, C.; Park, J.; Kim, M.; Kim, E.; Min, S. *Appl. Phys. Lett.* **1996**, *69*, 1924.
(8) Huang, F.; Wang, H.; Feldstein, M.; Macdiarmid, A.; Hsieh, B.; Epstein, A. *Synth. Met.* **1997**, *85*, 1283.

10.1021/cm035009p CCC: $27.50
Published on Web 02/03/2004

The question of surface functionalization for ALD is not generally well-understood, and it is particularly unstudied for the case of ALD of inorganic films on organic substrates. One serious issue that arises is the thermal stability of the polymer at the ALD process conditions. In the case of a SAM this is even more important because of the potential loss of ordering at elevated temperatures. Consequently, if it is desirable to maintain the ordering of the SAM during the growth of the ALD film, the ALD process must be done under conditions which are compatible with the thermal budget of the underlying polymer film.

One possible candidate for the ALD of a thin inorganic film on a SAM is the ALD of Al_2O_3 using trimethylaluminum [$Al(CH_3)_3$, TMA] because this ALD process has been demonstrated at temperatures as low as 30 °C.[10] Another advantage of Al_2O_3 is that it is thermodynamically stable and because of the strength of the Al−O and C−O bonds it can be used to enhance the adhesion of films to polymers. Furthermore, it is an excellent choice for a protective layer due to its stability and chemical inertness.[11] We have previously used DFT simulations to determine the chemical mechanisms for growing Al_2O_3 using both TMA[12] and trichloralaluminum [$AlCl_3$, TCA].[13] In this paper we use a similar approach to investigate the possibility of ALD of metal oxides on SAMs and the effect of SAM termination on the energetics of the ALD process.

Several different growth methods have been used to produce high-quality aluminum oxide films including reactive dc magnetron sputtering, molecular beam epitaxy (MBE), chemical vapor deposition (CVD), laser-assisted CVD, plasma-enhanced metal-organic CVD (PE-MOCVD), and ALD.[14−20] ALD has received considerable attention recently because the self-limiting nature of the process produces films that meet many of the requirements for growing films for microelectronics including atomic level control of thickness, which enables the growth of films with nanometer thicknesses, thickness uniformity over large areas, conformality, and low-temperature processing if the precursors react via chemical mechanisms with favorable kinetic and thermodynamic characteristics.

Among the various aluminum precursors, TMA is the most widely used due to its chemical simplicity, high vapor pressure (9 Torr at 20 °C), and highly exothermic reaction with H_2O. Other ALD chemistries for Al_2O_3 deposition have also been explored, including the TMA and ozone and TCA and water systems. Although the TMA/ozone system shows promise for growing high-quality alumina films, ozone oxidizes organic films and the TMA/ozone process temperature is high (350−450 °C).[21] Consequently, the TMA/ozone process is not chosen for this study. The TCA and water system is an industrial process that has been in use for quite some time. However, it requires relatively high temperatures (above 500 °C)[22] and is therefore not suitable for ALD on temperature-sensitive substrates, such as organic thin films. Furthermore, it produces HCl as a byproduct, which is incompatible with many materials due to its corrosiveness.

The atomistic mechanism of the ALD of Al_2O_3 using TMA and H_2O as reactants has been investigated previously by our group using density functional theory (DFT). We found that the metal precursor readily reacts with OH groups on an Al_2O_3 surface by first forming an adsorbed complex where a lone pair from the surface hydroxyl donates into the empty p orbital of the Al atom of the adsorbing TMA precursor to form a dative bond. This complex intermediate is relatively stable with an adsorption energy of 0.61 eV but not so stable that it traps the reaction at moderate temperatures, as is the case with ALD using TCA as the metal precursor.[12] The reaction proceeds by going through a four-centered transition state transferring the H of the surface OH group to a methyl ligand of the adsorbed TMA to form methane. The barrier for this step is approximately 0.52 eV relative to the complex intermediate, which is low enough that it should proceed at relatively low temperatures. The resulting product is an Al attached to the surface through an oxygen bridge with two methyl ligands. Thus, the first half-reaction replaces the hydroxyl termination of the surface with methyl termination. Furthermore, the overall reaction is exothermic by 1.70 eV.

The second half-reaction proceeds in a similar fashion. Water molecules adsorb onto the dimethylaluminum groups on the surface by donating a lone pair from the oxygen atom to the empty p orbital of the Al atom. The complex is 0.57 eV more stable than the initial state. A hydrogen atom of water then attacks a methyl ligand of the Al atom to form methane, exchanging the methyl ligand with an OH group. The barrier to this step is 0.70 eV relative to the water−$Al(CH_3)_2$ complex and overall the second half-reaction is exothermic by 1.48 eV. The low activation barriers and high exothermicity are consistent with the experimental observation that ALD of Al_2O_3 using TMA and water as precursors proceeds at low temperatures.[10]

We have also simulated growing Al_2O_3 using TCA and water as ALD precursors.[13] The reaction pathway is similar to that of the TMA case, although the complex intermediates are substantially more stable, and the activation barriers between the complexes and products are substantially higher. This is consistent with experimental observations that growth of Al_2O_3 using TCA requires significantly higher temperatures (above 500 °C) than needed for ALD using TMA.[22] On the basis of experimental observations and our own theoretical

(9) Arias, A.; Granstrom, M.; Thomas, D.; Petritsch, K.; Friend, R. *Phys. Rev. B* **1999**, *60*, 1854.
(10) Groner, M. D.; Fabreguette, F. H.; Elam, J. W.; George, S. M. *Chem. Mater.*, in press.
(11) Choy, K. *Prog. Mater. Sci.* **2003**, *48*, 57.
(12) Widjaja, Y.; Musgrave, C. *Appl. Phys. Lett.* **2002**, *80*, 3304.
(13) Heyman, A.; Musgrave, C. Submitted.
(14) Shih, K.; Dove, D. *J. Vac. Sci. Technol. A* **1994**, *12*, 321.
(15) Sawada, K.; Ishida, M.; Nakamura, T.; Ohtake, N. *Appl. Phys. Lett.* **1988**, *52*, 1672.
(16) Zborowski, J.; Golding, T.; Forrest, R.; Marton, D.; Zhang, Z. *J. Vac. Sci. Technol. B* **1998**, *16*, 1451.
(17) Ishida, M.; Katakabe, I.; Nakamura, T.; Ohtake, N. *Appl. Phys. Lett.* **1988**, *52*, 1326.
(18) Solanki, R.; Ritchie, W.; Collins, G. *Appl. Phys. Lett.* **1983**, *43*, 454.
(19) Kang, C.; Chun, J.; Lee, W. *Thin Solid Films* **1990**, *189*, 161.
(20) Ott, A.; Klaus, J.; Johnson, J.; George, S. *Thin Solid Films* **1997**, *292*, 135.
(21) Kim, J.; Chakrabarti, K.; Lee, J.; Oh, K.; Lee, C. *Mater. Chem. Phys.* **2003**, *78*, 733.
(22) Yun, S.; Lee, K.; Skarp, J.; Kim, H.; Nam, K. *J. Vac. Sci. Technol. A* **1997**, *15*, 2993.

results, we expect that TMA is a generally better precursor for ALD of Al_2O_3 on SAMs because its lower activation barriers and corresponding faster kinetics lead to lower ALD processing temperatures. Furthermore, the methane byproduct is more compatible with the growth chamber materials and metal and metal oxide ALD films than HCl produced by the TCA/water process.

To achieve selective ALD of the metal oxide film on the SAM, functionalized long-chain hydrocarbon SAMs on metal oxide or semiconductor surfaces might be used. The headgroups of the SAM molecules are anchored to the substrate and the end groups project away from the substrate such that the SAM surface consists of an ordered two-dimensional array of the SAM end group chemical functionality. The terminal functionality can be chemically or photochemically modified to alter the chemical composition, reactivity, and physical characteristics of the monolayer.[23] The structure is stabilized by van der Waals interactions between the alkyl chains. The ease of control of the chemical functionality of the surface of the SAM and the ability to pattern SAMs using microcontact printing have proven important in the fabrication of rational nanodevices.[24] Although there have been recent reports of the deposition of TiO_2 on patterned SAMs by an aqueous sol−gel deposition technique,[25,26] gas-phase deposition methods, such as ALD, have the advantages of better thickness control and homogeneity.

We report here for the first time a theoretical investigation of ALD on organic films involving the initial chemical reaction of TMA with SAMs terminated with different functional groups. The chemically adsorbed TMA can be used as the substrate for subsequent ALD reactions. This concept combines both the advantages of ALD and SAMs and might be a promising method for selective deposition of ultrathin oxide films. Furthermore, it provides information as to what functional groups may be compatible with ALD of Al_2O_3 in general, and specifically for ALD on SAMs for the purpose of area-selective ALD of metal oxides.

Despite its importance, a detailed understanding of the principles governing the effect of surface functionalization for ALD is not well-developed. This is particularly true for ALD on polymers and SAMs. Here, we investigate the effect of three different functional end groups, −OH, $-NH_2$, and $-CH_3$, on the ALD of Al_2O_3 to determine the effect of the end group on the formation of complex states and the ligand exchange reactions to create the initial ALD monolayer of TMA on the functionalized SAM surface.

Theoretical Calculations

We use the B3LYP hybrid DFT method to investigate the atomistic mechanisms, thermochemistry, and kinetics for the reaction of TMA with SAMs terminated with different end groups. B3LYP uses Becke's B88 gradient correction to exchange and the Slater and exact exchange functionals[27] along with the VWN and LYP correlation functionals.[28] The electronic structure is expanded over the 6-311++G(d,p) basis set placed on all atoms. Frequency calculations on stable structures and transition states yield zero-point energy (ZPE) corrections and confirm the nature of the stationary states. Furthermore, vibrational frequencies are used to construct the vibrational partition functions used in determining the preexponential factors for the rate equations using canonical transition state theory. All of the calculations are performed using the Gaussian 98 suite of programs.[29]

Because electronic structure calculations are computationally intensive, even with B3LYP DFT, which scales approximately as the cube of the system size in practice, we use a cluster to represent the chemically active portion of the SAM tail. This assumes that the chemical interactions which affect the relative energies of the reaction are localized. This assumption can be tested by using larger models of the surface. For simplicity, an ethyl group (CH_3CH_2) is used to represent the tail of one SAM chain. We have used a larger five-carbon atom [$CH_3(CH_2)_4$] alkyl chain to determine whether the chain length used to model the SAM affects the predicted energetics described below. To investigate the effects of different functional groups on the energetics of the reaction, CH_3CH_2OH, $CH_3CH_2NH_2$, and $CH_3CH_2CH_3$ clusters are used to represent $-OH$-, $-NH_2$-, and $-CH_3$-terminated SAM surfaces, respectively (Figure 1).

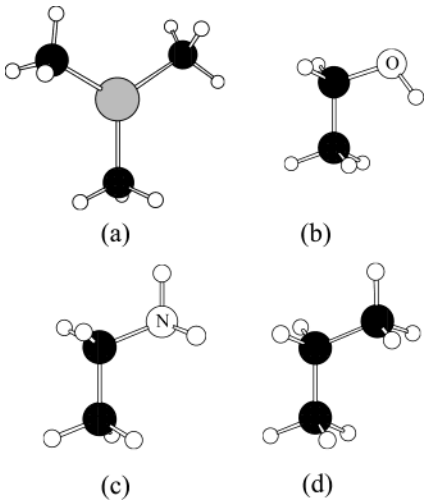

Figure 1. Cluster models used in the calculations. (a) TMA, (b) CH_3CH_2OH representing −OH group-terminated SAM, (c) $CH_3CH_2NH_2$ representing $-NH_2$ group-terminated SAM, and (d) $CH_3CH_2CH_3$ representing $-CH_3$ group-terminated SAM. The black, gray, white, ⓞ, and Ⓝ atoms denote carbon, aluminum, hydrogen, oxygen, and nitrogen atoms, respectively.

Results and Discussion

The potential energy surface (PES) of the reaction of TMA and the −OH-terminated SAM is shown in Figure 2. TMA first adsorbs molecularly onto the −OH site to form a complex with an adsorption energy of 0.60 eV.

(23) Schreiber, F. *Prog. Mater. Sci.* **2000**, *65*, 151.
(24) Fendler, J. *Chem. Mater.* **2001**, *13*, 3196.
(25) Koumoto, K.; Seo, S.; Sugiyama, T.; Seo, W.; Dressick, W. *Chem. Mater.* **1999**, *11*, 2305.
(26) Masuda, Y.; Jinbo, Y.; Yonezawa, T.; Koumoto, K. *Chem. Mater.* **2002**, *14*, 1236.
(27) Becke, A. *J. Chem. Phys.* **1993**, *98*, 5648.
(28) Lee, C.; Yang, W.; Parr, R. *Phys. Rev. B* **1988**, *37*, 785.
(29) Frisch, M. J.; Trucks, G. W.; Schlegel, H. B.; Scuseria, G. E.; Robb, M. A.; Cheeseman, J. R.; Zakrzewski, V. G.; Montgomery, J. A. J.; Stratmann, R. E.; Burant, J. C.; Dapprich, S.; Millam, J. M.; Daniels, A. D.; Kudin, K. N.; Strain, M. C.; Farkas, O.; Tomasi, J.; Barone, V.; Cossi, M.; Cammi, R.; Mennucci, B.; Pomelli, C.; Adamo, C.; Clifford, S.; Ochterski, J.; Petersson, G. A.; Ayala, P. Y.; Cui, Q.; Morokuma, K.; Malick, D. K.; Rabuck, A. D.; Raghavachari, K.; Foresman, J. B.; Cioslowski, J.; Ortiz, J. V.; Stefanov, B. B.; Liu, G.; Liashenko, A.; Piskorz, P.; Komaromi, I.; Gomperts, R.; Martin, R. L.; Fox, D. J.; Keith, T.; Al-Laham, M. A.; Peng, C. Y.; Nanayakkara, A.; Gonzalez, C.; Challacombe, M.; Gill, P. M. W.; Johnson, B.; Chen, W.; Wong, M. W.; Andres, J. L.; Gonzalez, C.; Head-Gordon, M.; Replogle, E. S.; Pople, J. A. *Gaussian 98*, revision A.5; Gaussian, Inc.: Pittsburgh, PA, 1998.

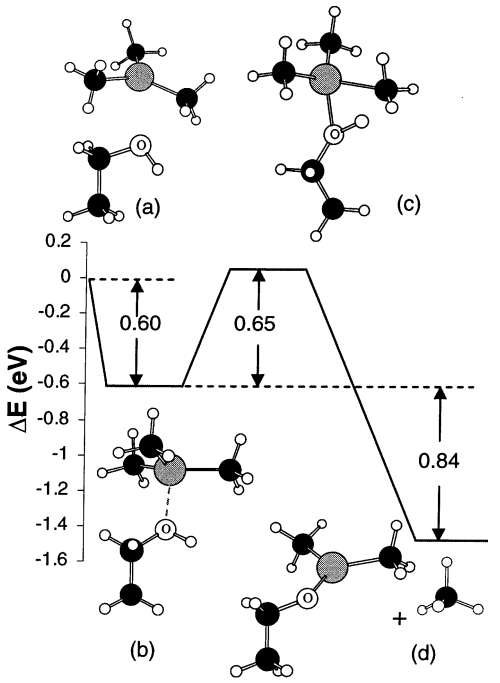

Figure 2. Reaction path and predicted energetics for reactions of TMA and −OH-terminated SAM. The stationary points correspond to (a) CH_3CH_2OH + TMA, (b) complex TMA·$OHCH_2CH_3$, (c) transition state, and (d) $CH_3CH_2O-Al(CH_3)_2$ + CH_4.

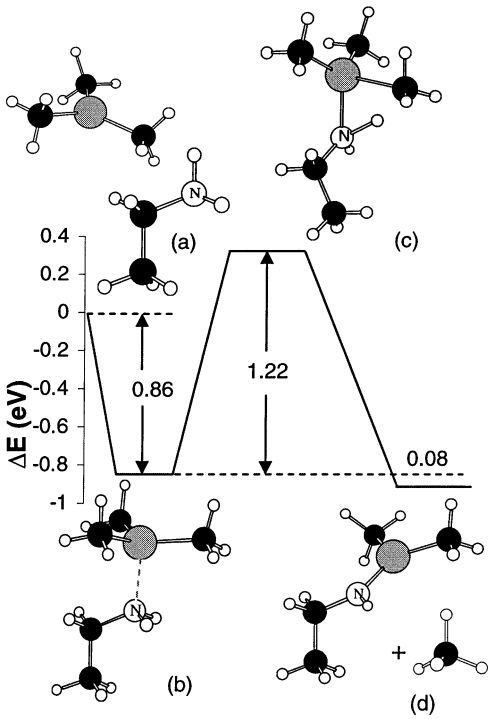

Figure 3. Reaction path and predicted energetics for reactions of TMA and $-NH_2$-terminated SAM. The stationary points correspond to (a) $CH_3CH_2NH_2$ + TMA, (b) complex TMA·$NH_2CH_2CH_3$, (c) transition state, and (d) $CH_3CH_2NH-Al(CH_3)_2$ + CH_4.

The molecular adsorption is an example of a Lewis acid−base interaction, with a group III alkyl (TMA) acting as the Lewis acid and a group VI hydride (OH) acting as the Lewis base. From our previous calculations of TMA and an −OH-terminated Al_2O_3 surface, a complex with similar structure and energetics (0.61 eV adsorption energy) is observed, indicating that the electron transfer occurring during formation of the dative bonded structure involves very local interactions. Subsequently, this complex can transfer the H atom from the hydroxyl group to the methyl ligand by undergoing a four-centered Al−O−H−C transition state with an activation barrier relative to the complex intermediate of 0.65 eV. The optimized geometry for the product is shown in Figure 2. The gas-phase byproduct of this reaction is methane (CH_4), which is not bound to the surface and thus desorbs on formation. In contrast, in the case of ALD using TCA, the HCl byproduct forms a bond to the surface and not only requires some energy to desorb but also can re-adsorb and block surface sites for further adsorption of the precursor, which leads to slower growth rates as well as incorporation of chlorine into the film and film nonuniformity. This is another advantage of using TMA as the metal precursor over using the metal chloride. Furthermore, methane is more compatible with reactor materials than HCl.

In the case of SAM termination with an $-NH_2$ group (Figure 3), the reaction pathway is qualitatively similar to the reaction with the −OH group-terminated SAM and similarly involves the formation of a complex intermediate. However, the relative energies are significantly different, leading to a somewhat qualitatively different potential energy surface. First, the adsorption energy is 0.86 eV. Sauls et al. obtained a value of 0.84 eV experimentally, which corresponds well with our calculation.[30] Consequently, the Al−N dative bond that forms is 0.25 eV stronger than the Al−O dative bond resulting from TMA adsorption at hydroxyl sites. Adsorption is then followed by CH_4 formation and desorption, with a reaction barrier of 1.22 eV and a reaction energy of 0.08 eV, both relative to the complex. The reaction barrier relative to the adsorbed complex is nearly twice as large as the barrier of the analogous reaction on the −OH-terminated SAM (0.65 eV). These results indicate that the intial reaction on an $-NH_2$-terminated SAM will require higher temperatures to overcome the larger activation barrier for ligand exchange.

A simple kinetic analysis assuming the pre-exponential factors are the same for both cases shows that the amine-terminated SAM must be heated to 333 °C to achieve the same reaction rate as TMA on hydroxyl-terminated SAMs at 30 °C. This temperature is well above the disordering temperature of the SAM. An alternative would be to use lower temperatures which would require longer exposures of the SAM to the precursor since the kinetics favor desorption of the precursor over reaction to form the ALD ligand exchange products. Here, we assume the reaction temperature for TMA on −OH-terminated SAM is only 30 °C since ALD has been demonstrated at 30 °C and we obtain similar reaction energetics for TMA on the −OH-terminated SAM and on the as-grown Al_2O_3 surface, which further indicates that the ALD surface chemistry is quite local.

(30) Sauls, F. C.; Interrante, L. V.; Jiang, Z. *Inorg. Chem.* **1990**, *29*, 2989.

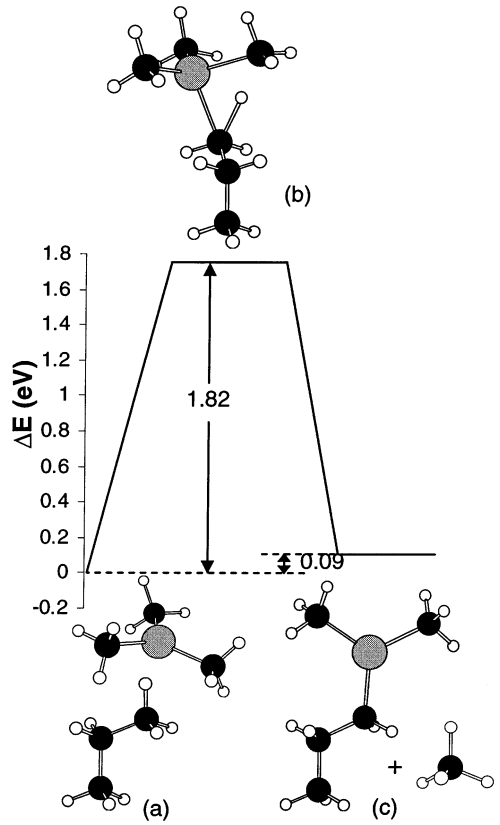

Figure 4. Reaction path and predicted energetics for reactions of TMA and $-CH_3$-terminated SAM. The stationary points correspond to (a) $CH_3CH_2CH_3$ + TMA, (b) transition state, and (c) $CH_3CH_2CH_2-Al(CH_3)_2$ + CH_4.

Table 1. Comparison of Proton Affinity, Activation Barrier, and Total Energy for SAMs with Different Termination

	−OH	$-NH_2$	$-CH_3$
H^+ affinity	13.90	14.89	17.85
barrier	0.65	1.22	1.82
total energy	−1.44	−0.94	0.09

For the case of the $-CH_3$-terminated SAM (shown in Figure 4), our theoretical calculations predict that no intermediate complex structure is formed because there are no electron lone pairs in the pure alkane chain to act as a Lewis base for TMA to bind to. On the other hand, a four-centered Al−O−H−C transition state is formed, connecting the TMA and SAM reactants with the dimethylaluminum-terminated SAM and a gas-phase CH_4 byproduct. Not only does no complex form in this case, but also the reaction barrier is the highest (1.82 eV) of the three cases studied here. The overall enthalpy of reaction relative to the reactants is 0.09 eV *endothermic*, which suggests that the reaction of TMA with the $-CH_3$-terminated SAM is not energetically favorable and thus there is no thermodynamic driving force for the ALD reaction to take place on the pure alkane chain.

The overall initial reaction on the SAM can be regarded as the production of methane from an active H and $-CH_3$ of the SAM functional groups and TMA, respectively. Table 1 shows a comparison of proton affinities, calculated reaction energies, and activation barriers of TMA with different end group-terminated SAMs. We find that the proton affinity increases from −OH to $-NH_2$ with $-CH_3$ being the largest. This trend

Table 2. Bond Energies (eV)

	C−H	O−H	N−H	Al−C	Al−O	Al−N
$Al(CH_3)_3$				3.26		
$CH_3CH_2CH_3$	4.19					
CH_3CH_2OH		4.30				
$CH_3CH_2NH_2$			4.13			
CH_4	4.40					
$CH_3CH_2Al(CH_3)_2$				2.99[a]		
$CH_3CH_2OAl(CH_3)_2$					4.62	
$CH_3CH_2NHAl(CH_3)_2$						3.93

[a] C is from the SAM chain.

explains the lowest reaction energy for the −OH-terminated SAM among the three end groups. The activation barrier increases similarly from −OH to $-NH_2$ to $-CH_3$. The calculated trends in activation energies are consistent with Hammond's postulate, which states that the activation energy decreases when the reaction is more exothermic, although here the reaction on the $-CH_3$-terminated SAM has a different reaction coordinate.[31] Also calculated are the selected bond energies involved in the ligand exchange reaction, which we list in Table 2. On the basis of the bond energies, we expect that the product of TMA with the −OH-terminated SAM will be the most thermodynamically stable, as shown by the reaction enthalpy, because these bond energies should predict the reaction energy, neglecting the effects of the surrounding material. The total reaction energy can be expressed in terms of bond energies:

$-CH_3$-terminated SAM:

$$\Delta E \cong E_{\text{bond}}(\text{Al}-\text{C in TMA}) + E_{\text{bond}}(\text{C}-\text{H in } CH_3CH_2CH_3) - E_{\text{bond}}(\text{Al}-\text{C in product}) - E_{\text{bond}}(\text{C}-\text{H in } CH_4) = 0.07 \text{ eV}$$

−OH-terminated SAM:

$$\Delta E \cong E_{\text{bond}}(\text{Al}-\text{C in TMA}) + E_{\text{bond}}(\text{O}-\text{H in } CH_3CH_2OH) - E_{\text{bond}}(\text{Al}-\text{O in product}) - E_{\text{bond}}(\text{C}-\text{H in } CH_4) = -1.46 \text{ eV}$$

$-NH_2$-terminated SAM:

$$\Delta E \cong E_{\text{bond}}(\text{Al}-\text{C in TMA}) + E_{\text{bond}}(\text{N}-\text{H in } CH_3CH_2NH_2) - E_{\text{bond}}(\text{Al}-\text{N in product}) - E_{\text{bond}}(\text{C}-\text{H in } CH_4) = -0.94 \text{ eV}$$

This simple bond energy analysis of the active bonds of the ligand exchange reaction predicts the reaction energies on the functionalized SAMs almost exactly and predict that the −OH-terminated SAMs have the largest thermodynamic driving force for reaction with TMA and by Hammond's postulate likely the lowest reaction barrier among the three terminal groups studied here. This analysis depends on the extent of the effects of the surrounding material, which we have found to be generally small for all the cases we have investigated.[12,32−34]

(31) Lowry, T. H.; Richardson, K. S. *Mechanism and Theory in Organic Chemistry*, 3rd ed.; Harper Collins: New York, 1987.
(32) Kang, J.; Musgrave, C. *J. Appl. Phys.* **2002**, *91*, 3408.
(33) Widjaja, Y.; Musgrave, C. *Appl. Phys. Lett.* **2002**, *81*, 304.
(34) Widjaja, Y.; Musgrave, C. *J. Chem. Phys.* **2002**, *117*, 1931.

Table 3. Reaction Energies for −OH-Terminated SAM and TMA (Energies Are Relative to the Sum of the Reactant Energies)

energy (eV)	2 carbon atom chain	5 carbon atom chain
complex	−0.60	−0.61
reaction barrier	0.66	0.67
products	−1.44	−1.45

Table 4. Selected Bond Lengths (Å)

	Al−N	Al−O	N−H	O−H	Al−C
TMA					1.97
CH_3CH_2OH				0.96	
$CH_3CH_2NH_2$			1.01		
CH_3CH_2OH-TMA (complex)		2.06		0.96	1.99
$CH_3CH_2NH_2$-TMA (complex)	2.11		1.02		2.00
$CH_3CH_2O-Al(CH_3)_2$ (product)		1.72			1.96
$CH_3CH_2NH-Al(CH_3)_2$ (product)	1.80				1.97

To investigate whether the ethyl group is sufficient to represent the alkyl chain of the SAM, we also calculate the ALD reaction energetics for the larger $CH_3(CH_2)_4$ OH cluster, which includes three additional CH_2 monomer units of the SAM alkane chain. The reaction mechanism is found to be the same as that found using the smaller cluster (CH_3CH_2OH). The results are shown in Table 3. The energy differences for all states are on the order of 0.01 eV from the results using the shorter alkyl model described above. This suggests that the reaction of TMA with SAMs with different functional group termination is highly localized and the length of the alkyl chain has almost no effect on the selective adsorption of TMA. Consequently, the smaller cluster of CH_3CH_2-R (R: SAM end group) is a good model for the investigation of the SAM termination chemistry for ALD since it is sufficiently large to describe the surface reactions accurately.

Reactions of TMA with both the −OH-terminated SAM and $-NH_2$-terminated SAM involve the formation of complexes between the TMA precursor and the surface-active sites. To enable formation of a dative bond between two molecules, the central atom in one molecule must have a lone pair of electrons and the central atom of the other molecule must be short a pair of valence electrons. Here, DFT calculations yield a stable TMA structure with planar geometry, which is consistent with gas-phase electron diffraction data.[35,36] This implies that one Al 3s orbital and two Al 3p orbitals hybridize to form three sp^2 orbitals to bond to the three CH_3 groups, leaving an empty p orbital on the Al atom. This empty orbital can accept one lone pair of electrons from the O atom of the −OH or N atom of $-NH_2$ to form a dative-bonded complex.

Another characteristic feature of dative bonding is that dative bonds are relatively long compared to covalent bonds. To illustrate the physical changes that accompany bonding to the surface, Table 4 lists a number of the selected bond lengths for the free TMA molecule, the TMA·$OHCH_2CH_3$ dative-bonded complex, the TMA·$NH_2CH_2CH_3$ dative-bonded complex, the $CH_3CH_2OAl(CH_3)_2$ product, and the $CH_3CH_2NHAl(CH_3)_2$ product. The dative-bonded complex in Figure 2 has an Al−O bond length of 2.06 Å. This is 0.34 Å longer than the 1.72 Å Al−O bond length calculated for the $CH_3CH_2OAl(CH_3)_2$ product. Bonding of TMA to the surface lengthens the Al−C bonds slightly (from 1.97 to 1.99 Å), but does not change the O−H bond length. These changes in structure are accompanied by changes in charge distribution within the molecule. The natural population analysis (NPA) method is used to analyze the charge distributions.[37] In NPA, the populated molecular orbitals are decomposed into their individual atomic orbital components, permitting assignment of charge to individual atomic centers. The effective charge on the TMA is −0.12 e when dative-bonded to the OH surface.

The changes in bond lengths on reaction are similar for the reaction of TMA and the NH_2-terminated SAM. The TMA·$NH_2CH_2CH_3$ dative-bonded complex has a Al−N bond length of 2.11 Å, which is 0.31 Å longer than the Al−N bond length in the $CH_3CH_2NHAl(CH_3)_2$ product. Similarly, dative bonding of TMA to the surface lengthens the Al−C bonds from 1.97 to 2.00 Å. The effective charge on TMA in the adsorbed complex is −0.16 e. This result is expected because oxygen (Pauling electronegativity of 3.44) is more electronegative than nitrogen (3.04), and consequently the effective charge on TMA in the TMA·$NH_2CH_2CH_3$ complex should be larger than that in the TMA·$OHCH_2CH_3$ complex. Furthermore, in the bond energy calculations, the dative bond in TMA·$NH_2CH_2CH_3$ is significantly stronger than that of TMA·$OHCH_2CH_3$ because the amine group contributes more electron density than the hydroxyl group in forming dative bonds.

Rate constants (s^{-1}) of these adsorption reactions are calculated using conventional transition state theory (TST).[38] The TST rate expression is given by

$$k(T) = \sigma \frac{k_b T Q^{\neq}(T)}{hQ(T)} \exp\left(-\frac{E^{\neq}}{k_b T}\right)$$

where the symmetry factor σ gives the reaction path multiplicity (that is, the number of equivalent paths over which reactants can reach products) and Q and $Q^{\neq}$ are the overall partition functions of the reactants and transition state, respectively. The quantity $E^{\neq}$ represents the energy of the saddle point relative to the reactants. Data required to calculate the partition functions include rotational constants, harmonic frequencies, and energetics, which are obtained using the DFT method described above.

Here, we assume the TMA complex formation is fast as the adsorption reaction through the formation of the dative bond is barrierless because no bond breaking takes place. Furthermore, we assume that energy transfer from the reactants into the reaction coordinate is inefficient. Thus, the vast majority of the TMA molecules do not proceed over the reaction barrier without first becoming dative bonded to the surface. Consequently, we treat the complex as the reactant for the following kinetic analysis. The rate coefficients for each reaction were calculated for seven temperatures in the range of 200−700 K and then fitted to an

(35) Almennin*, A.; Halvorse*, S.; Haaland, A. *Acta Chem. Scand.* **1971**, *25*, 1937.
(36) Huffman, J.; Streib, W. *J. Chem. Soc., Chem. Commun.* **1971**, 911.
(37) Reed, A.; Weinstock, R.; Weinhold, F. *J. Chem. Phys.* **1985**, *83*, 735.
(38) Computational Science and Engineering Online (CSEO), http://www.cseo.net.

Table 5. Rate Constant (s^{-1}) for the Reactions of −OH-, $-NH_2$-, and $-CH_3$-Terminated SAM and TMA at Different Temperatures

temperature (K)	−OH	$-NH_2$	$-CH_3$
200	1.53×10^{-5}	1.95×10^{-20}	$1.14 \times {}^{-63}$
250	3.94×10^{-2}	5.03×10^{-14}	1.94×10^{-54}
298	6.19	6.90×10^{-10}	1.86×10^{-48}
400	5.07×10^{3}	2.21×10^{-4}	1.95×10^{-40}
500	2.54×10^{5}	3.74×10^{-1}	1.10×10^{-35}
600	3.46×10^{6}	5.41×10^{1}	1.82×10^{-32}
700	2.24×10^{7}	1.91×10^{3}	3.92×10^{-30}
A	9.16×10^{11}	6.93×10^{10}	9.37×10^{-24}
n	0.08	0.54	2.28
E_a	0.67	1.26	1.79

Arrhenius-like form, $k(T) = AT^n \exp(-E_a/RT)$, which are shown in Table 5. We have not included the effect of hydrogen tunneling, which may enhance the reaction rate at low temperatures.

For the reaction between TMA and the −OH-terminated SAM, we obtain the following rate equation:

$$k(T) = 9.16 \times 10^{11}\, T^{0.08} \exp(-7.81 \times 10^{3}/T)$$

For the reaction between TMA and $-NH_2$-terminated SAM, we obtain the rate equation:

$$k(T) = 6.92 \times 10^{10}\, T^{0.54} \exp(-1.46 \times 10^{4}/T)$$

And finally, for the reaction between TMA and $-CH_3$-terminated SAM, we obtain the rate equation

$$k(T) = 9.37 \times 10^{-24}\, T^{2.28} \exp(-2.08 \times 10^{4}/T)$$

At room temperature, the rate constant of the −OH-terminated SAM is 6.19 s^{-1}, which is 10 orders of magnitude higher than that of the $-NH_2$-terminated SAM (6.90×10^{-10} s^{-1}), and 48 orders higher than that of the $-CH_3$-terminated SAM (1.86×10^{-48} s^{-1}). As expected, the reaction of TMA on −OH-terminated SAMs is predicted to be significantly faster than with amine or methyl termination. These results indicate that TMA will selectively adsorb on both the −OH- and $-NH_2$-terminated SAMs but not on the $-CH_3$-terminated SAM. The ligand exchange reactions of the three terminations are highly selective as indicated above: TMA will react to form products at low temperatures on −OH-terminated SAMs but not on $-NH_2$-terminated SAMs. At moderate temperatures, the ligand exchange reaction will take place for the $-NH_2$-terminated SAMs but not the $-CH_3$-terminated SAMs. This selectivity of ALD on SAMs with different functionalization could be used to pattern Al_2O_3 into desired patterns. First, SAMs with selected functional end groups can be patterned on the substrate by microcontact printing. Subsequently, TMA can be selectively adsorbed on the SAM or uncovered substrate depending on the affinity of the functional group toward TMA. Finally, ALD can be performed on the adsorbed state to grow uniform, thin Al_2O_3 films.

The ALD growth of Al_2O_3 using TMA and H_2O as precursors can be separated into two half-reactions,

$$Al{-}OH^* + Al(CH_3)_3 \rightarrow Al{-}O{-}Al{-}(CH_3)_2{}^* + CH_4 \quad (1)$$

$$Al{-}CH_3{}^* + H_2O \rightarrow Al{-}OH^* + CH_4 \quad (2)$$

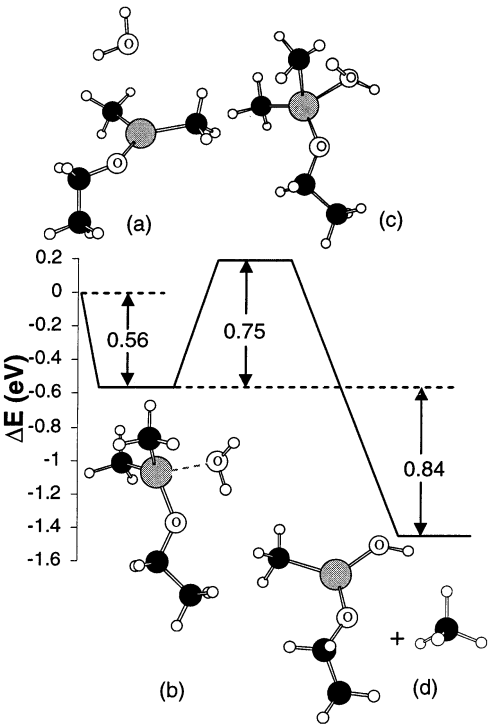

Figure 5. Reaction path and predicted energetics for reactions of H_2O and the product from the reaction between TMA and −OH-terminated SAM. The stationary points correspond to (a) $CH_3CH_2OAl(CH_3)_2 + H_2O$, (b) complex $H_2O{\cdot}Al(CH_3)_2OCH_2$-$CH_3$, (c) transition state, and (d) $CH_3CH_2O{-}AlCH_3OH + CH_4$.

where the asterisks denote the surface species. We have described the reactions for the first half-reaction with the functionalized SAM above. Here, we describe the results for the second half-reaction and show the PES in Figure 5. H_2O first adsorbs by forming a complex with the $C{-}O{-}Al{-}CH_3$ site. This step is exothermic by 0.56 eV and produces CH_4, which desorbs from the surface. This reaction has an activation energy of 0.75 eV relative to the complex state and the reaction is exothermic by 1.40 eV. The mechanism of this second half-reaction of ALD growth of Al_2O_3 is the same as predicted previously for ALD of Al_2O_3. Because the energy difference is less than 0.1 eV, these reactions are quite localized and the reaction mechanism can be generalized. We have also calculated the second half-reaction of water with TMA dative-bonded to the amine functional group. We do not find a stable complex nor a low-energy ligand exchange reaction for this case, indicating that, at low and moderate temperatures, the ALD reactions on the amine-functionalized SAMs do not proceed beyond the TMA dative-bonded state. This is expected because TMA has only one empty valence orbital, and thus the capacity to form only one dative bond. Furthermore, we found in the first half-reaction that the ligand exchange reaction for the amine has a large activation barrier.

Conclusions

In conclusion, the surface reactions between TMA and SAMs terminated with different functional groups are investigated using DFT. Our results show that the reaction of TMA and the −OH-terminated SAM is favored both thermodynamically and kinetically over

the reaction with $-NH_2$- and $-CH_3$-terminated SAMs. Reactions on the $-NH_2$-terminated SAM form more stable complex intermediates; however, because the ligand exchange barrier is large, the precursors are trapped in the adsorbed complex state. Furthermore, although there is a thermodynamic driving force for this reaction, the reaction is relatively slow compared to the $-$OH-terminated case and desorption of the precursor is favored over ligand exchange. In the case of the $-CH_3$-terminated SAM, there is no thermodynamic driving force for the reaction and the reaction barrier is large. The energetics of the reactions do not depend on the length of the SAM using ethyl and pentyl groups as models. After the initial TMA adsorption on the $-$OH-terminated SAM, the second half-reaction of ALD growth of Al_2O_3 ($Al-CH_3^* \rightarrow Al-OH^*$) is calculated and the mechanism and energetics are consistent with our previous results for ALD of Al_2O_3 using TMA and water.[11] Because these adsorption reactions are highly localized, these conclusions are not only limited to the effect of surface functionalization on ALD reactions on SAMs; they can also be extended to reactions on other substrates and to ALD reactions involving other precursors which form dative-bonded complexes.

Acknowledgment. The authors thank Collin Mui and Joseph Han for their assistance and Steven George for helpful discussions. Support of this work through an Office of Naval Research MURI is gratefully acknowledged.

CM035009P